To be published in Optics Express:

Title:	Decay rate enhancement of diamond NV-centers on diamond thin films
Authors:	Hao Li,Jun-Yu Ou,Vassili Fedotov,Nikitas Papasimakis
Accepted:	24 June 21
Posted	24 June 21
DOI:	https://doi.org/10.1364/OE.425706

Decay rate enhancement of diamond NV-centers on diamond thin films

HAO LI,* JUN-YU OU, VASSILI A. FEDOTOV AND NIKITAS PAPASIMAKIS

Optoelectronics Research Center & Center for Photonic Metamaterials, University of Southampton, Southampton SO17 1BJ, UK
**H.Li@soton.ac.uk*

Abstract: We demonstrate experimentally two-fold enhancement of the decay rate of NV^0 centers on diamond/Si substrate as opposed to a bare Si substrate. We link the decay enhancement to the interplay between the excitation of substrate modes and the presence of non-radiative decay channels. We show that the radiative decay rate can vary by up to 90% depending on the thickness of the diamond film.

1. Introduction

The nitrogen-vacancy (NV) defect in diamond constitutes an important test ground and building block for quantum devices [1-7]. Structured plasmonic films, dielectric and plasmonic particles, epsilon-near-zero media and hyperbolic metamaterials are known to enhance decay rates of quantum emitters owing to the Purcell effect [8-16]. Charge transfer from silicon and metallic substrates provides an additional mechanism to control NV center emission [17], while the sensitivity of NV centers to the local dielectric environment has been used for mapping of local density of states [18] and near-field microscopy [19]. However, the NV center decay rates are broadly distributed, which hinders studies of their interactions with their environment [20, 21].

In this paper, we report a two-fold increase of the decay rate for ensembles of NV^0 emitters resting on a thin diamond film, as compared to a bare silicon substrate, which we observed experimentally using time-resolved cathodoluminescence (TR-CL). We attribute such an increase to the existence of non-radiative channels and coupling of the emitters to Fabry-Perot modes of the thin film.

2. Experimental design and results

In our experiments, we considered ~120 nm large nanodiamonds containing ~10^3 NV centers. The nanodiamonds were diluted in methanol and the solution was mixed for 10 min in an ultrasonic bath. The nanodiamonds were then deposited by drop casting on two different substrates: a 200 nm thick diamond film on silicon and a bare silicon wafer (see Fig. 1(b)). We characterized NV centers in the deposited nanodiamonds at room temperature using a scanning electron microscope (SEM) operating in fixed-spot mode. The electron beam was incident on the samples through a small hole in a parabolic mirror, which collected and collimated the emitted light. The collected light was subsequently directed to the entrance of a VIS/NIR spectrometer, as shown in Fig. 1(a). The spectrometer selected photons within a 3.6 nm wavelength range around the central wavelength of 575 nm and directed them to the input of a single photon detector. The beam blanker driven with a wave function generator produced a pulsed electron beam and also provided the synchronization required to implement time-correlated single-photon counting [22]. The NV centres are excited by an electron pulse with duration t_D=1.5 µs. The pulse repetition rate is 500 kHz, which corresponds to 2 µs with a switch-off time for the e-beam of t_{off} = 500 ns. During measurements, the beam current and electron energy are maintained at ~1.8 nA and 10 kV, respectively. The system can measure reliably lifetimes as short as ~3 ns (see also Supplement 1, Section S1).

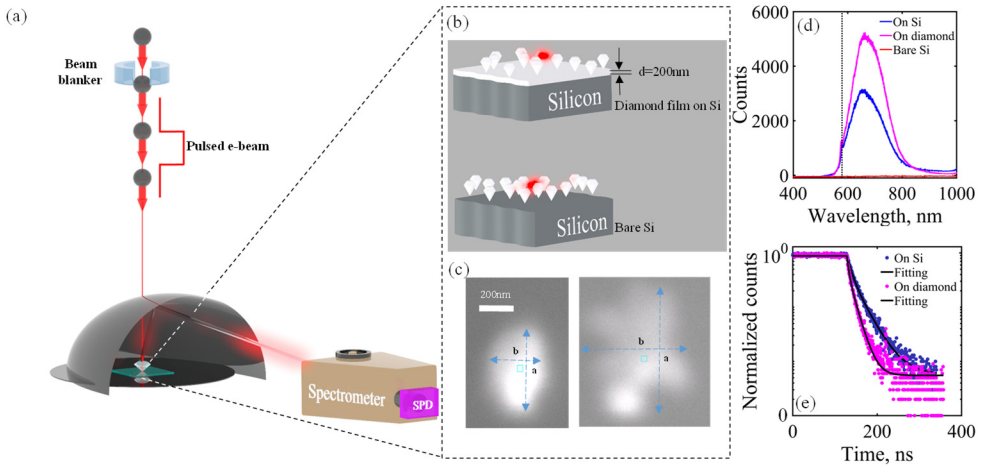

Fig. 1. (a) Schematic of the scanning electron microscope-based system for time-resolved electron-induced light emission spectroscopy. Electrons impinge on the sample through a small hole in a parabolic mirror, which collects and collimates the emitted light. The beam is subsequently directed to the spectrometer. At the output of the spectrometer, a single photon detector (SPD) is used to detect the emitted photons. (b) The samples consist of NDs deposited on two different substrates: i) a 200 nm thick diamond film on 500 μm thick silicon and ii) a 500 μm thick silicon substrate. (c) SEM images of two different ND clusters (left and right). The ND clusters consist of different number of NDs resulting in different cluster sizes. The blue rectangle marks the position of the electron beam on the ND clusters during TR-CL measurements. The dimensions of the cluster are indicated by the longer and shorter edge lengths, a and b, respectively. (d) CL spectrum of NV centers on Si (blue), on diamond film (magenta) and background signal from the bare Si substrate (red). The vertical dashed line marks the position of the zero phonon line. (e) TR-CL traces of NV center emitters on Si (blue), on diamond film (magenta), while the black lines correspond to bi-exponential fittings.

We selected 60 nanodiamond clusters on each type of substrate with sizes in the range 120-1500 nm. The size of the clusters was calculated as $(a+b)/2$, where a and b are the longer and shorter dimensions of the cluster, respectively (see Fig. 1(c)). We studied the emission of the neutral NV^0 centers at the zero phonon line, as shown in Fig. 1(d). Thus, only photons in the range of 575 $\pm$ 1.8 nm were selected at the input of the single photon detector. The CL emission from the bare Si substrate (in absence of NV centers) was negligible (see red line in Fig. 1(d)) compared to the emission from NV centers on both substrate types (see blue and magenta lines in Fig. 1(d)). Typical decay traces of NV centers on Si and on diamond are presented in Fig. 1(e), where it is evident that in the latter case the CL emission decays considerably faster. The photon counting histograms were fitted using the following formula:

$$I = a_1(1-\delta(t+a_2)) + 0.5a_1\delta(t+a_2)(e^{-\frac{t+a_1}{\tau_1}} e^{-\frac{t+a_2}{\tau_2}}) + a_3 \quad (1)$$

where $\boldsymbol{a_1}$ is the normalized peak photon number, $\boldsymbol{a_2}$ is the sample irradiation time, $\boldsymbol{a_3}$ is the background noise, the faster characteristic time, $\boldsymbol{\tau_1}$, is related to the carrier time [23], while the slower $\boldsymbol{\tau_2}$ corresponds to the NV center lifetime.

Figures 2(a-b) present the distribution of the measured lifetimes of NV centers deposited on a bare Si substrate and on a diamond film, respectively. We characterized the statistical distribution of the lifetimes by the corresponding average (μ) and the standard deviation (σ). NV centers on bare Si substrate are seen to exhibit long lifetimes (μ=30 ns) and a broad distribution (σ=6 ns). On the other hand, for NV centers on the diamond film, we observe a substantial shortening of the average lifetime (μ=17 ns) accompanied by a narrower distribution (σ=4 ns).

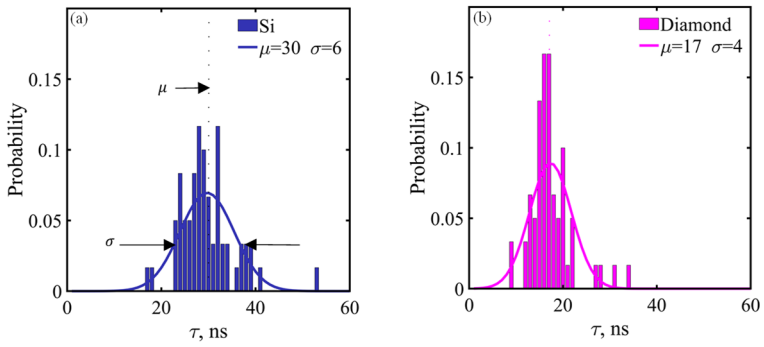

Fig. 2. Lifetime distributions of NV^0 centers in diamond nanoparticles deposited on silicon (a) and on diamond thin film on silicon (b). The histograms are obtained from measurements of 60 different ND clusters on each substrate and are fitted by a Gaussian distribution, where μ is the mean (dotted vertical lines) and σ is the standard deviation (in ns).

3. Discussion

We argue that the changes in the lifetime distribution observed for NV centers on a diamond film are a result of strong interactions between diamond nanoparticles and guided optical modes in the diamond film. To demonstrate this we performed full-wave 3D electromagnetic modeling of the emission from a dipole embedded in a diamond nanoparticle placed on a diamond film of varying thickness. The modeling also allowed us to distinguish between radiative and non-radiative decay channels. A comparison of computationally obtained and experimentally measured total lifetimes is presented in Table 1. In agreement with our experimental results, our simulations show that the lifetime is shorter in the presence of a thin diamond film (81 ns) than in the case of a bare Si substrate (91 ns). We attribute the difference between the values of experimental and numerical lifetimes mainly to the fact that in our numerical calculations we considered single nanodiamond particles, whereas experimental measurements involved clusters of nanodiamonds. In particular, our numerical results indicate that the faster decay rates obtained for thin diamond films are due mainly to non-radiative loss in the underlying bulk Si (see Supplement 1, Table S1). Importantly, the enhancement or suppression of radiative and non-radiative decay rate depends strongly on the film thickness (see Fig. 3(a)), which indicates coupling to slab modes in the film [24]. Indeed, at the thickness of the experimentally measured samples (90 nm) radiative (non-radiative) decay rates are suppressed (enhanced), whereas at 160 nm film thickness the situation is reversed. This is further illustrated in radiated field maps plotted in Figs. 3(b) and 3(c) for the film thickness of 90 nm and 160 nm, respectively. The modelled dependence of the radiative decay rate on the film thickness can be fitted with a sine function: $k + l\sin(\omega x + m)$, as shown in Fig. 3 (a). From the fitting parameters we obtain the period of the sine function, $T^{\mathrm{rad}}_{\mathrm{diamond}} = \frac{2\pi}{\omega^{\mathrm{rad}}_{\mathrm{diamond}}}$ =126 nm, which is close to the thickness of a diamond film supporting the fundamental Fabry-Perot mode at λ=575nm: $T^{\mathrm{FP}}_{\mathrm{diamond}} = \frac{575\ \mathrm{nm}}{2n_{\mathrm{diamond}}}$ = 120 nm. We, therefore, conclude that the decay rate can be efficiently controlled by changing the thickness of the supporting thin film. In particular, the tuning depth of NV radiative decay rate for a thin diamond film can be as high as $\frac{2l^{\mathrm{rad}}_{\mathrm{diamond}}}{k^{\mathrm{rad}}_{\mathrm{diamond}}}$ = 89%, where $l^{\mathrm{rad}}_{\mathrm{diamond}}$ and $k^{\mathrm{rad}}_{\mathrm{diamond}}$ are the fitting parameters of the sine function.

We argue that in our study the average lifetime is largely independent of the inhomogeneities in the substrate and immediate dielectric environment, as well as NV emitter position and orientation of its electric dipole moment. Indeed, the large number of NV emitters per particle yields a Purcell factor effectively averaged over different positions and dipole

orientations of the emitters in nanodiamonds. Moreover, our experimental measurements indicate that the NV center lifetimes are almost independent on the ND cluster size and shape for both types of substrates, indicating that the observed differences in decay rates originate primarily from emitter-substrate interactions (Supplement 1, Section S2). The NV emission spectra can be characterized by six parameters, corresponding to the peak value, peak position, and linewidth of the zero phonon line (ZPL) and phonon sideband (PSB). In our measurements, the peak position of the ZPL and PSB varied weakly with the cluster size on the order of $\pm$2% or smaller, which we attribute to the differences in the strain and electrostatic environment of each cluster. On the other hand, the corresponding linewidths exhibited considerable dependence on cluster size, which we argue is due to inhomogeneous broadening. Finally, the levels of peak emission also varied strongly with cluster size as a result of the excitation of a larger number of NV centers in larger ND clusters.

Table 1. Experimentally measured ($\bar{\tau}_{Exp}$) and numerically simulated (τ_{Sim}) NV center total lifetimes on diamond film and bare silicon substrate. Experimental values correspond to the average of the distribution.

Substrates	$\bar{\tau}_{Exp}(ns)$	$\tau_{Sim}(ns)$
Si	30	91.49
Diamond	17	81.73

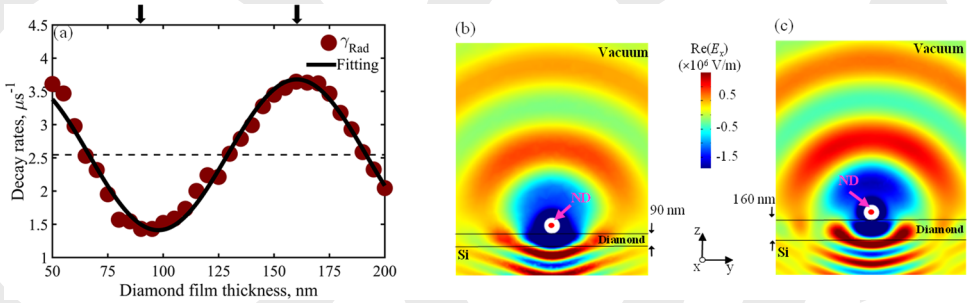

Fig. 3. (a) Modelled radiative decay rates of an NV center on a diamond film as a function of the film thickness. The electric dipole moment of the emitter is oriented parallel to the plane of the substrate. The solid line corresponds to a sine function fit to the numerically calculated decay rates (solid circles), while the dashed line corresponds to the radiative decay rate of an NV center on a bare silicon substrate. (b-c) The real part of x-component of the electric field emitted in zy-plane by an NV center of a nanodiamond (ND) sitting on a diamond film with a thickness of 90 nm and 160 nm, respectively (the electric dipole moment of the NV center is oriented along x-axis).

4. Conclusion

In conclusion, we experimentally demonstrate two-fold enhancement of the decay rate of NV^0 centers in nanodiamonds when deposited on a thin diamond film. We attribute the enhancement to the presence of non-radiative decay channels and coupling of NV^0 centers to the optical slab modes supported by the film, which leads to increase of both radiative and non-radiative decay rates. As such, we show that varying the thickness of the diamond film allows tuning of the radiative decay rate by up to 90%. Our study provides insights into the mechanism of Purcell enhancement of NV emission from nanodiamonds deposited on thin films and puts forward simple means of controlling the corresponding emission statistics.

Funding. Engineering and Physical Sciences Research Council (Grants No. EP/M0091221) and China Scholarship Council (No. 201608440362).

Disclosures. The authors declare no conflicts of interest.

Data availability. Following a period of embargo, the data from this paper can be obtained from the University of Southampton repository at: http://doi.org/10.5258/SOTON/D1823.

Supplemental document. See Supplement 1 for supporting content.

References

1. S. M. C. Kurtsiefer, P. Zarda, and H. Weinfurter, "Stable Solid-State Source of Single Photons," Phys Rev Lett **85** (2000).
2. A. B. R. Brouri, J.-. Poizat, and P. Grangier, "Photon antibunching in the fluorescence of individual color centers in diamond," Optics Letters **25** (2000).
3. K. M. C. Fu, C. Santori, P. E. Barclay, I. Aharonovich, S. Prawer, N. Meyer, A. M. Holm, and R. G. Beausoleil, "Coupling of nitrogen-vacancy centers in diamond to a GaP waveguide," Applied Physics Letters **93** (2008).
4. A. Huck, S. Kumar, A. Shakoor, and U. L. Andersen, "Controlled coupling of a single nitrogen-vacancy center to a silver nanowire," Phys Rev Lett **106**, 096801 (2011).
5. J. T. Choy, I. Bulu, B. J. M. Hausmann, E. Janitz, I. C. Huang, and M. Lončar, "Spontaneous emission and collection efficiency enhancement of single emitters in diamond via plasmonic cavities and gratings," Applied Physics Letters **103** (2013).
6. I. Aharonovich, and E. Neu, "Diamond Nanophotonics," Advanced Optical Materials **2**, 911-928 (2014).
7. H. Siampour, S. Kumar, and S. I. Bozhevolnyi, "Nanofabrication of Plasmonic Circuits Containing Single Photon Sources," ACS Photonics **4**, 1879-1884 (2017).
8. M. B. S. Schietinger, T. Aichele, and O. Benson, "Plasmon-Enhanced Single Photon Emission from a Nanoassembled Metal-Diamond Hybrid Structure at Room Temperature," Nano Lett **9**, 1694-1698 (2009).
9. K. Tanaka, E. Plum, J. Y. Ou, T. Uchino, and N. I. Zheludev, "Multifold enhancement of quantum dot luminescence in plasmonic metamaterials," Physical review letters **105**, 227403 (2010).
10. J. T. Choy, B. J. M. Hausmann, T. M. Babinec, I. Bulu, M. Khan, P. Maletinsky, A. Yacoby, and M. Lončar, "Enhanced single-photon emission from a diamond–silver aperture," Nature Photonics **5**, 738-743 (2011).
11. S. Kumar, A. Huck, and U. L. Andersen, "Efficient coupling of a single diamond color center to propagating plasmonic gap modes," Nano Lett **13**, 1221-1225 (2013).
12. M. Y. Shalaginov, S. Ishii, J. Liu, J. Liu, J. Irudayaraj, A. Lagutchev, A. V. Kildishev, and V. M. Shalaev, "Broadband enhancement of spontaneous emission from nitrogen-vacancy centers in nanodiamonds by hyperbolic metamaterials," Applied Physics Letters **102** (2013).
13. S. K. H. Andersen, S. Kumar, and S. I. Bozhevolnyi, "Ultrabright Linearly Polarized Photon Generation from a Nitrogen Vacancy Center in a Nanocube Dimer Antenna," Nano Lett **17**, 3889-3895 (2017).
14. S. I. Bogdanov, M. Y. Shalaginov, A. S. Lagutchev, C. C. Chiang, D. Shah, A. S. Baburin, I. A. Ryzhikov, I. A. Rodionov, A. V. Kildishev, A. Boltasseva, and V. M. Shalaev, "Ultrabright Room-Temperature Sub-Nanosecond Emission from Single Nitrogen-Vacancy Centers Coupled to Nanopatch Antennas," Nano Lett **18**, 4837-4844 (2018).
15. A. S. Zalogina, R. S. Savelev, E. V. Ushakova, G. P. Zograf, F. E. Komissarenko, V. A. Milichko, S. V. Makarov, D. A. Zuev, and I. V. Shadrivov, "Purcell effect in active diamond nanoantennas," Nanoscale **10**, 8721-8727 (2018).
16. J.-K. So, G. H. Yuan, C. Soci, and N. I. Zheludev, "Enhancement of luminescence of quantum emitters in epsilon-near-zero waveguides," Applied Physics Letters **117**, 181104 (2020).
17. S. Stehlik, L. Ondic, A. M. Berhane, I. Aharonovich, H. A. Girard, J.-C. Arnault, and B. Rezek, "Photoluminescence of nanodiamonds influenced by charge transfer from silicon and metal substrates," Diamond and Related Materials **63**, 91-96 (2016).
18. A. W. Schell, P. Engel, J. F. Werra, C. Wolff, K. Busch, and O. Benson, "Scanning single quantum emitter fluorescence lifetime imaging: quantitative analysis of the local density of photonic states," Nano Lett **14**, 2623-2627 (2014).
19. J. Tisler, T. Oeckinghaus, R. J. Stohr, R. Kolesov, R. Reuter, F. Reinhard, and J. Wrachtrup, "Single defect center scanning near-field optical microscopy on graphene," Nano Lett **13**, 3152-3156 (2013).
20. A. Mohtashami, and A. Femius Koenderink, "Suitability of nanodiamond nitrogen–vacancy centers for spontaneous emission control experiments," New Journal of Physics **15** (2013).
21. H. Lourenço-Martins, M. Kociak, S. Meuret, F. Treussart, Y. H. Lee, X. Y. Ling, H.-C. Chang, and L. H. Galvão Tizei, "Probing Plasmon-NV0 Coupling at the Nanometer Scale with Photons and Fast Electrons," ACS Photonics **5**, 324-328 (2017).
22. R. J. Moerland, I. G. Weppelman, M. W. Garming, P. Kruit, and J. P. Hoogenboom, "Time-resolved cathodoluminescence microscopy with sub-nanosecond beam blanking for direct evaluation of the local density of states," Opt Express **24**, 24760-24772 (2016).
23. M. Sola-Garcia, S. Meuret, T. Coenen, and A. Polman, "Electron-Induced State Conversion in Diamond NV Centers Measured with Pump-Probe Cathodoluminescence Spectroscopy," ACS Photonics **7**, 232-240 (2020).
24. M. A. Schmidt, D. Y. Lei, L. Wondraczek, V. Nazabal, and S. A. Maier, "Hybrid nanoparticle-microcavity-based plasmonic nanosensors with improved detection resolution and extended remote-sensing ability," Nat Commun **3**, 1108 (2012).